Chain of algorithms to calculate advanced radiation parameters

Jan Remund, Lucien Wald, John Page

Remund J., Wald L., Page, J., 2003. Chain of algorithms to calculate advanced radiation parameters. Proceedings of ISES Solar World Congress, 16-19 June, Göteborg, Sweden, CD-ROM published by International Solar Energy Society

CHAIN OF ALGORITHMS TO CALCULATE ADVANCED RADIATION PARAMETERS

Jan Remund
METEOTEST, Fabrikstrasse 14, CH-3012 Bern, Switzerland,
+41 (0)31 3072626, +41 (0)31 3072610, e-mail: remund@meteotest.ch

Lucien Wald
Ecole des Mines de Paris /Armines, Groupe Teledetection & Modelisation, BP 207, F-06904 Sophia Antipolis cedex , France

John Page
Emeritus Professor of University of Sheffield, Building Science, Sheffield S11 9BG, United Kingdom

Abstract – Algorithms linked to form focused chains of algorithms are needed to fill gaps between often measured or available data resources and the parameters requested by many solar applications. This paper describes the formulation of a chain of algorithms for shortwave radiation. The basic inputs into the chain are monthly mean values of the Linke turbidity factor and global radiation. The outputs of the chain are hourly values of global shortwave radiation on inclined planes. This is achieved via stochastic generation of daily and hourly values of global radiation, splitting the global into beam and diffuse radiation and finally calculating the radiation on inclined planes. The cloudless sky chain is based on an improved version of the clear sky model of Rigollier et al. (2000). The stochastic generation process is based on Aguiar et al. (1988, 1992) but important improvements have been made by cross-linking to the clear sky model. The Perez models (1986, 1990) are used for splitting the radiation into its components and for estimating radiation on tilted planes. Datasets produced with the described chains can be accessed via the prototype of the SoDa project at www.soda-is.org.

1. INTRODUCTION

This paper depicts the chain of algorithms for generating, hour by hour, day by day, shortwave radiation. It shows their integration in a compound service like SoDa (Wald et al., 2002).

Existing models were used as far as possible. The main scientific contributions emerged through the systematic inter-comparison of the ESRA (2000) and METEONORM (2000) (Remund et al., 1998) chains leading onto the definition of a new standard in the modelling of solar radiation parameters, by using the best of both existing chains and filling gaps by focused research.

The basic inputs to the full chain are monthly mean values of the Linke turbidity factor and global radiation. The outputs of the chain are hourly values of global radiation on inclined planes. This is achieved via stochastic generation of daily and hourly values of global radiation by splitting global radiation into beam and diffuse radiation and finally calculating the radiation on inclined planes. The stochastic process leads to an hourly dataset of a statistically average year with average mean, minimum and maximum values.

2. DEFINITION OF CHAINS

Algorithms linked to form focused chains of algorithms are needed to fill gaps between generally available data resources and the parameters requested by solar applications. This report first describes the parameters needed to address applications. Then the algorithms are established and linked into defined chains to provide the requested information from the available inputs.

Based on measurements and/or interpolation worldwide monthly mean values of global radiation and other meteorological parameters are available. Unfortunately, most applications need hourly time series of at least global radiation. This information gap can be filled with an algorithmic chains resource. The missing parameters are mainly values that are not stored (too many values), not available (not public) or not measured (needing too complicated equipment).

The main missing parameter is the global radiation on inclined planes. The diffuse radiation part is needed to calculate this value. Frequently only monthly values of climatic data are available only for certain parts of the world, so techniques to generate hourly values world wide are required.

Tab. 1: Proposed models for chain of algorithms. Models not used in ESRA or METEONORM are highlighted (bold).

Model	Algorithms	ESRA	METEONORM	SoDa
Solar geom.	div.	Bourges (1985)	Ineichen (1983)	Bourges (1985)
Clear sky	Beam	Rigollier et al. (2000)	Rigollier et al. (2000)	**Rigollier corr.**
	Diffuse	Rigollier et al. (2000)	Global-Beam	**Rigollier corr.**
	Global	Global + Diffuse	Kasten 1983	Global + Diffuse
Daily profile	Global	Collares-P. and Rabl, (1979)	Gueymard (2000)	**New**
Stochastic gener.	Global day	-	Aguiar et al. (1988)	**Aguiar et al. (1988) corr.**
	Global hour	-	Aguiar & Collares-Pereira (1992)	**Aguiar & Collares-Pereira (1992) corr.***
Rad. Separation	Diffuse	ESRA (2000)	Perez et al. (1991)	**Perez et al. (1991)**
Tilted planes	Global	Muneer (1990)	Perez et al. (1986/87)	Perez et al. (1986/87)
High horizons	Global	-	Remund et al. (1998)	Remund et al. (1998)

* Aguiar and Collares-Pereira: only stochastic part (profile by other model)

The following description is concentrated on new or corrected models, the changes in clear sky models are described in the paper "Worldwide Linke turbidity information". Additional parameters like temperature and dewpoint temperature also available in SoDa are not described in this paper.

3. THE ESTIMATION OF HOURLY VALUES OF SHORT WAVE RADIATION

The basic inputs into the short wave chain of algorithms used to estimate the hourly values of the irradiance in the new system are monthly values of global radiation Gm and the air mass 2 Linke turbidity factor TL.

The target of this chain of algorithms is to provide hourly values of global, diffuse and beam radiation on horizontal and inclined planes. The whole chain does not have to be used for all applications. It is possible to run only parts of the chain. This choice is dependent on input data availability and the precise output data requirements.

This process is complemented by the use of state-of-the-art models for splitting the global radiation into its beam and diffuse components. A state of art model for predicting hour by hour radiation on inclined planes provides the last link in the chain.

4. DAILY VALUES OF GLOBAL RADIATION

The model of Aguiar et al. (1988) provided the starting point for this new methodology. This Markov chain model is included in METEONORM (no model of this type is used in ESRA). It calculates daily values of G_d with monthly mean values of G_m as inputs. A change in this model was implemented in the new process:

The original model gives one single distribution of daily clearness index KT_d values for any one monthly mean value KT_m (see definition in Annex). The model does not take into account any local factors like site altitude above sea level (higher maximum irradiation values at higher altitude) or different turbidity situations. There are also problems with the coupling to the clear sky model of ESRA when this original model is used in the new chain of algorithms. The estimated clear sky values can be much higher or much lower than the maximum values predicted by the unmodified Aguiar. The whole system of the matrices was therefore changed from a clearness index basis to clear sky clearness index basis. Formulated like this, the maximum value of $KT_{d,c}$ (=1) must correspond automatically to the clear sky model predictions used. $KT_{d,c}$ is calculated as the ratio $G_d/G_{c,d}$.

The mapped resource of monthly mean Linke turbidity factors is used to drive the clear sky model to obtain the required monthly mean daily values of $G_{c,d}$ needed to calculate $KT_{d,c}$ in any selected month for any point**.** This change required the daily Markov transition matrices tables to be completely revised to match the new formulation. The new Tables giving the revised distributions are given in the Annex. The description of the methodology can be found at Aguiar et al. (1998).

4.1 Validation

The validation was done at 10 stations. 3 stations are in Switzerland, 3 in Germany, 1 in Puerto Rico and 3 in the USA. The stations cover a wide range of climates. As a measure of quality, the root mean square error (RMSE) between measured and generated kt values was calculated. The mean bias errors (MBE) are small.

In order to calculate the mean daily profiles of the measured values, the daily values were binned in KT_d groups using a 0.05 band width.

The new RP model shows the smallest deviation from the measured values at most stations and the best overall result for all sites. The model ACP has the highest deviations. CPRG-model is second best. This model is very similar to CPR, showing slightly better results at higher latitudes (Tab. 2).

Tab. 2: RMSE of hourly KT_h values (generated – measured). The best model is highlighted. ACP: Aguiar & Collares-Pereira (1992); GM: Gueymard (2000); CPR: Collares-Pereira & Rabl (1979); CPRG: Collares-Pereira & Rabl (1979), Gueymard (2000).

Site	Latitude	Period	ACP	GM	RP	CPR	CPRG
Magadino	46°10'N	95 - 99	0.094	0.071	**0.067**	0.070	0.070
Haerkingen	47°19'N	95 - 99	0.102	**0.087**	0.093	0.088	0.088
Hamburg	53°39'N	81 - 90	0.055	0.046	0.047	**0.044**	**0.044**
Würzburg	49°46'N	81 - 90	0.062	0.040	**0.038**	0.039	**0.038**
Weihenstephan	48°24'N	81 - 90	0.064	0.039	**0.036**	0.041	0.040
Albuquerque	35°03'N	61 - 90	0.091	0.076	**0.048**	0.063	0.062
Dodge City	37°46'N	61 - 90	0.098	0.081	0.088	0.074	**0.073**
San Juan	18°26'N	61 - 90	0.082	0.077	**0.055**	0.066	0.066
Anchorage	61°10'N	61 - 90	0.105	0.077	**0.068**	0.083	0.082
All sites			0.095	0.078	**0.072**	0.075	0.0074

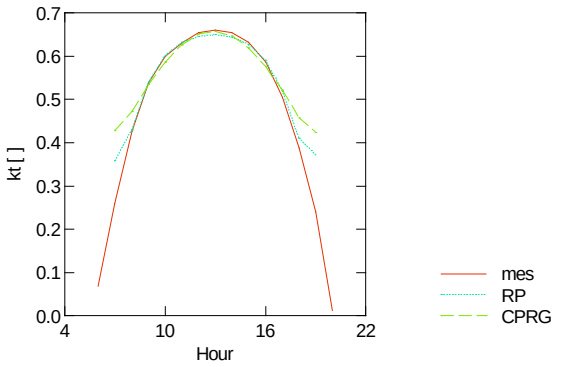

Fig. 1: Mean daily profiles of KT_h for daily KT_d values of 0.6 at San Juan PR.

Fig. 1 shows typical forms of the profiles. At noon all lines are very close. At low solar altitude the measured values are lower than the modeled ones; the new model is in between the measurements and the values of the model used in ESRA. Further, significantly higher KT_h values are measured and calculated for very low solar altitudes. The new model quite often yields – as do the measured values – higher KT_h values for the first and the last hour of the day. This is due to the one dimensional concept of the clearness index, where, as in nature, the radiation – particularly at low solar elevation – is influenced by the three dimensional form of the atmosphere. To avoid unreasonable values, the KT_h values are limited to values of 0.8 for solar elevation below 10°.

The new model has the advantage of allowing good interaction with the SoDa/ESRA clear sky model.

5. HOURLY VALUES OF SHORTWAVE RADIATION

5.1 Generating mean daily profiles of irradiance.

Knowledge of the mean daily profiles is essential for many simulation applications. It is also the first step in the generation of hourly values of global radiation from daily values of clearness index.

The model of Aguiar and Collares-Pereira (1992) was used in METEONORM Version 3.0 (Remund and Kunz, 1997). This model is very badly suited for high latitudes. The hourly integration model of Gueymard (2000) was introduced in version 4 of METEONORM (Remund and Kunz, 1999). Gueymard validated different models for 135 stations. One of them was the model of Collares-Pereira and Rabl (1979), which is used in ESRA (2000). Gueymard also presented a corrected version of Collares-Rabl model, that was better adapted for high latitudes. Gueymard's new model and the corrected model of Collares-Rabl showed approximately the same quality.

Method. For the new chain of algorithms we included another model based on the hypothesis that the average day global irradiance mean profile should exactly mirror the clear day global profile in form. The proposed method for mean daily irradiance profile generation is therefore based on the use of the global radiation clear sky profile to calculate the global irradiance profile for all days in the time series.

$$G_h = G_d \cdot \frac{G_c}{G_{c,d}} \qquad (2)$$

where G_d is the daily global horizontal irradiance, G_c the clear sky hourly global irradiance, $G_{c,d}$ the daily

clear sky global irradiance. Other authors like Grüter et al. (1986) have used this approach as well.

The advantage of this model is that daily values of beam or diffuse radiation do not have to be known in advance. The model, called Remund-Page (RP) here, fits perfectly to the upper edge of the distribution, i.e. the clear sky profile, which is needed as a first step in the chain of algorithms. A short validation can be found in the next section.

Validation. The model was validated at 12 sites (Tab. 3 and 4). The distributions (Fig. 2), the first auto-correlation and the maximum KT_d value were investigated. The maximum values are dependent on the T_L values used and the quality therefore on the accuracy of the T_L.

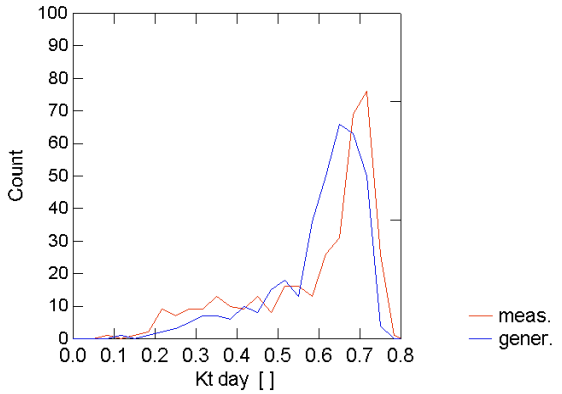

Fig. 2: Histogram of the daily KT_d values for Dodge City (USA).

The validation does not show a clear result. Generally the new model is slightly better (Tab. 3 and 4). The distributions do not differ much from the original ones. Generally the new model shows better results for North American sites than for European sites. This could be explained by the choice of sites used for making the original and the new model.

Tab. 3: Correlation coefficients of the grouped frequencies (width of groups: 0.05) as a measure of the quality of the distribution (better model is highlighted).

Site	Original	New
Raleigh	0.897	**0.910**
Dodge City	0.766	**0.773**
Int. Falls	0.715	**0.854**
Salt Lake City	0.910	**0.939**
Haerkingen	**0.693**	0.645
Hamburg	0.854	**0.884**
Würzburg	0.796	**0.814**
Weihenstephan	**0.881**	0.763
Nice	**0.973**	0.933
Kobenhavn	**0.895**	0.886
Arhangelsk	**0.781**	0.715
Mean	**0.769**	0.754

Whatever the relative results look like, only the new version allows a good interaction with the clear sky model. Additionally the new model is easier to use (no minimum and maximum classes) and generally runs faster (less loops).

Tab. 4: First autocorrelation of daily KT_d values.

Site	Meas-ured	Original	New
Raleigh	0.406	**0.321**	0.306
Dodge City	0.335	0.153	**0.301**
Int. Falls	0.332	0.261	**0.387**
Salt Lake City	0.456	0.358	**0.524**
Haerkingen	0.542	0.344	**0.403**
Hamburg	0.447	**0.383**	0.381
Würzburg	0.471	0.275	**0.351**
Weihenstephan	0.512	0.313	**0.325**
Nice	0.346	0.292	**0.339**
Kobenhavn	0.422	**0.402**	0.387
Arkangelsk	0.459	0.358	**0.479**
mean difference	-	-0.125	**-0.060**
Standard error	-	**0.071**	0.085

5.2 Stochastic generation of hourly variations in global irradiance from the daily mean profile

The stochastic generation of hourly irradiance values from the daily mean profile is based on the model of Aguiar and Collares-Pereira (1992) (TAG-model: **T**ime dependent, **A**uto-regressive, **G**aussian model). This model, also used in METEONORM, consists of two parts: the first part calculates an average daily profile. No change has been made to this model compared to Remund et al. (1998), so we refer to this paper.

5.3 Splitting the global radiation to diffuse and beam

The models of Perez (METEONORM) and Skartveit (Satel-light project) for the splitting of global radiation have been examined briefly. The models are very similar after the correction of Skartveit (1998). The disadvantage of using a model like Perez or Skartveit is that the hourly diffuse values can not be known without (stochastic) generation of hourly global values. Therefore the beam and diffuse values depend to a small extent on random numbers. The use of mean daily profiles to calculate the beam and diffuse profile is not reliable. Both the Skartveit and Perez models depend on the hourly variations from one hour to the next. Mean profiles and hourly values with variations do not give the same result.

One advantage of the Skartveit model is that a correction for high albedoes is available for this model. There is also a formula to calculate the hourly variation, if this value is not known. The model was adapted to data of Bergen, Norway. The Perez model, which is more widely used, is still the standard model.

It can be adapted to both US and EU climates. A model has been included in the SoDa chains to estimate the hourly variation parameter dk for use with the Perez model for cases in which no hourly variation data are available:

$$\begin{aligned} &KT_{h,c} \le 0.98 \\ &dk = 0.1 - 0.03 * \sin\left[\left(KT_{h,c} - 0.05\right)\cdot 8.527\right] \\ &- 0.02 \cdot KT_{h,c} \\ &KT_{h,c} > 0.98 \\ &dk = -1.634 + 1.72 \cdot KT_{h,c} \end{aligned} \quad (6)$$

Tab. 5: Results of the comparison of Perez and Skartveit model. "mod." means modelled variance from hour to hour (according to Eqn. 6).

Site	Perez	Perez mod.	Skartv.	Skartv. mod.	Perez	Perez mod.	Skartv.	Skartv. mod.
	MBE	MBE	MBE	MBE	RMSE	RMSE	RMSE	RMSE
Payerne BSRN 1998	**-0.7**	3.7	5.5	6.5	34.5	44.5	**33.9**	43.0
Vaulx-en-Velin IDMP 1994	**10.2**	12.5	12.1	13.9	38.1	41.8	**36.0**	40.3
Melbourne (Australia) 1998	**3.2**	10.5	11.0	11.3	**43.1**	49.4	43.2	46.3

Validation. A short validation of the models was made at 3 sites (Tab. 5). The quality of the different models is about the same with some advantages for Perez. Our decision to use the Perez model has been influenced by the possibility of using it with high horizons (Remund et al., 1998). The introduction of the modeling of the hourly variations lowers the accuracy of both models.

5.4 Radiation on the inclined plane

The Perez model (Perez et al. 1986) enables global and diffuse radiation to be calculated on an inclined surface using two input values, hourly global horizontal and diffuse horizontal irradiance.

The diffuse radiation on an inclined surface is calculated as the sum of two diffuse components, diffuse celestial irradiance (D_i^c) and diffuse reflected irradiance (D_i^r) by means of Eqn. 7:

$$G_i = B_i + D_i^c + D_i^r \quad (7)$$

The beam component is simply given by

$$B_i = B_n \cdot \cos(\theta) \quad (8)$$

The diffuse reflected irradiance (D_i^r) is calculated with the following model:

$$D_i^r = \underbrace{\frac{1-\cos(\beta)}{2}}_{r_g} \cdot (\rho \cdot G_h) \quad (9)$$

where β is the surface inclination, r_g the isotropic reflected view factor and ρ the surface albedo. As no changes have been made, we refer to Remund et al. (1998).

New albedo model. The albedo is calculated with a model that gives albedo as a function of temperature. A new model is introduced. Verification with 8 stations showed that the model of Brühwiler (1990) is not sufficient – especially in Swiss mountains, the place it has been made for. Data of GEBA (Goose, Fredericton, Jokmok, Toronto, Hamburg, Payerne) and WRC Davos (ASRB network Davos and Weissfluhjoch) were used for adapting and testing the new model.

$$\begin{aligned} &\text{For areas with great amount of snow :} \\ &\rho = 0.618 - 0.044 \cdot \text{Ta} \quad , 0.2 \le \rho \le 0.8 \\ &\text{For the rest of the world :} \\ &\rho = 0.423 - 0.042 \cdot \text{Ta} \quad , 0.2 \le \rho \le 0.8 \end{aligned} \quad (10)$$

The r^2 values for both models are 0.92 and 0.93, respectively. A distinct separation for areas with a great amount of snow and areas with less snow was found. A great amount of snow enhances the possibility of fresh snow and therefore higher albedoes and prolongates the time of snow cover in spring. For temperatures below -10°C and above 10°C there is no difference between the models. The separation into the 2 groups is not easy. As a first approximation the following rule is used to determine areas with a great amount of snow:

- Sum of precipitation for 3 winter months > 150 mm
- Mean temperature for 3 winter months < -3°C

The new model gives very similar results to the model used in versions 3 and 4 in the range of 0.2–0.5 (Fig. 3). The big difference is for values greater than 0.5, which did not exist with the old model – but was found in the data.

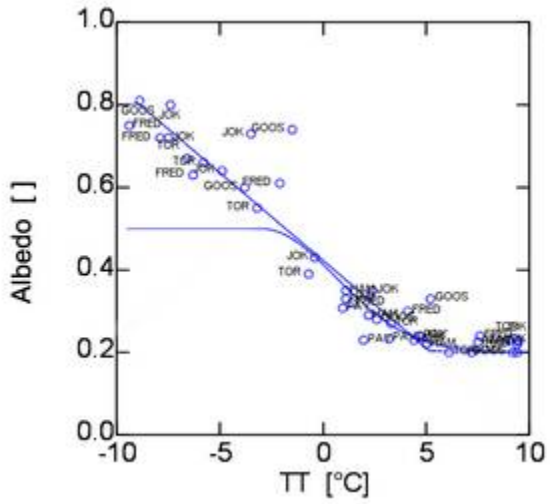

Fig. 3: Albedo vs. temperature (TT). Model used in version 3 and 4 (with max. at 0.5) and new model (max. at 0.8).

In various tests the following temperatures were evaluated to use for albedo calculation: With hourly generated data the mean of the last 2 weeks is used. If only monthly temperature values are available, the interpolated daily value of the day 5 days before is used.

Validation of the slope irradiance model. The generated diffuse radiation on inclined planes is calculated in two steps. The two Perez models were first tested alone with measured hourly values of global radiation as inputs. Secondly they were tested within the combined model, using generated hourly radiation values.

Validation was carried out for 2 sites in Switzerland for inclinations of 33–45° with a more or less South orientation (typical for solar energy applications) and also for a West facing facade in Bavaria (typical exposure for overheating studies using building simulation).

Tests of inclined surface data for solar energy applications

Using measured hourly global radiation values:

The tests were carried out for 2 sites in Switzerland with data of 1993 (Berne-Marzili, 46.95°N, 7.45°E, 520 m, inclination 35°, azimuth: 37°E; Locarno-Magadino: 46.18°N, 8.85°E, 197 m, inclination: 35°S, azimuth: 15°W). The average MBE error in the hourly values was 5 W/m^2 (over all hours) (generated values slightly too high) and the RMSE standard deviation 33 W/m^2 ($G_h > 0$). For monthly average values, the MBE was 3 W/m^2 (5 %) and the RMSE 5 W/m^2. The distributions of both MBE and RMSE errors display a distinct seasonal variation.

Using generated hourly values:

The tests were carried out for 2 sites in Switzerland. The average MBE error in the average monthly values was 0 W/m^2 (1 %) (generated values too high) and the RMSE standard deviation 5 W/m^2 (6 %). For yearly average values, the MBE was 2 W/m^2 (1 %) and the RMSE 5 W/m^2 (3 %). The average discrepancy with generated radiation is (surprisingly) somewhat smaller than achieved with measured radiation as input. This indicates that the errors partly compensate one-another. The distributions of both MBE and RMSE again display a distinct yearly pattern, having a maximum in winter.

Test for building simulation

Using measured hourly global radiation values:

The test was carried out at Holzkirchen (Bavaria; 11.71°E, 47.87°N, 680m) for a West facade. The average MBE error in the hourly values was 3 W/m^2 (over all hours) (generated values slightly too high) and the RMSE standard deviation 51 W/m^2 ($G_h > 0$). For monthly average values, the MBE was 3 W/m^2 (0 %) and the RMSE 8 W/m^2 (13 %).

Using generated hourly values:

The test was carried out at Holzkirchen on a West facade. The average MBE error in the average monthly valuesm^2 (7 %) (generated values too high) and the RMSE standard deviation 7 W/m^2 (9 %). The average discrepancy with generated radiation is somewhat bigger than with measured radiation as input. The distributions of both MBE and RMSE errors display a distinct yearly pattern, having a maximum in winter (as for tests in Switzerland).

5.5 Modification of irradiance due to horizon

The aim of the modification method described here is to calculate the radiation at sites with raised (distant) horizons. A number of assumptions which were used in the raised (local) skyline model are not valid in this case. The modification procedure for the different radiation components is described in this section.

For the modifications due to skyline profiles we also refer to Remund et al. (1998), as no changes were made.

6. CONCLUSIONS

New chains drawing on the design of the existing METEONORM chains with algorithms mainly selected from those used in ESRA were developed. Testing against observed data shows that the stochastic generation of the hourly short wave parameters is possible and that the quality is acceptable. The models constructed are based as much as possible on published work. Nevertheless some important new validated chain links were introduced.

The main scientific contributions sprang from the detailed inter-comparison of the ESRA and METEONORM chains. This process drove the achievement of a new standard in the modelling of solar radiation parameters for practical applications on a global basis, using the best of both existing chains.

The establishment of a well-defined functional relationship between clear day and all day short wave radiation models was especially important for systematic model building . This relationship could not have been made into an effective working tool without the extensive efforts made within the SoDa program to establish a world wide digitally mapped data resource of values of the Linke turbidity factors.

The understanding of the relationship between solar radiation estimation and screen air temperature estimation was advanced into effective working program that deliver data needed for effective simulation for any site in the world. Globalisation of the algorithmic structures was indeed achieved.

One drawback springing from lack of time in the face of many challenges within the framework of SoDa, is that not all parts of the chains could be reviewed with the same thoroughness. Therefore some parts, mainly at the end of the longer chains – like the radiation on inclined planes with high horizons – are used without validation.

The advanced chain of algorithms was included in the new version of METEONORM.

Acknowledgements - Many thanks goes to H. Gilgen and A. Ohmura of Institute for Atmosphere and Climate ETH (IACETH) for BSRN data and data of Payerne and Reckenholz.
The Swiss Agency for Environment, Forest and Landscape (SAEFL) provided data of 3 NABEL stations and the Australian Regional Instrument Center, Bureau of Meteorology a CD-ROM with global and beam irradiance data of several years.
Further we like to thank the Fraunhofer Institute for Building Physics IBP Holzkirchen for the example climate dataset as well as TNC (Erlenbach ZH) for global radiation data on inclined surfaces.
Swiss Meteorological Institute provided data of 5 ANETZ-stations.
This work is supported partly by the programme IST of the European Commission, by the Swiss Federal Office of Energy, Bern (conctract No. 79564) and the Swiss Federal Office for Education and Science (contract No. 99.0513).

REFERENCES

Aguiar, R., M., Collares-Pereira and J.P. Conde, 1988: A simple procedure for generating sequences of daily radiation values using a library of markov transition matrices. *Solar Energy, Vol. 40, No.3, pp. 269-279.*

Aguiar, R. and M. Collares-Pereira, 1992: TAG: A time-dependent auto-regressive, Gaussian model. *Solar Energy, Vol. 49, No.3, pp. 167-174.*

Aguiar R. and J.Page, 1998: Algorithm Manual of the ESRA Standard Set of Routines. European Solar Radiation Atlas Project, Contract JOU2-CT)*-305. INETI, Dep. Renewable Energies, Lisbon.

Bourges, B., 1985. Improvement in solar declination calculations. *Solar Energy*, Vol.35, pp.367-369. 1985.

Collares-Pereira M. and Rabl A., 1979. The average distribution of solar radiation: Correlations between diffuse and hemispherical values. *Solar Energy*, Vol. 22, 155-164.

ESRA, 2000. European Solar Radiation Atlas, ESRA. Les Presses de l'Ecole de Mines. Paris 2000.

Gruter W., H. Guillard, W. Möser, J.M.Monget, W. Palz, E. Raschke, R.E. Reinhardt, P.Schwarzmann, L. Wald, 1986. Solar Radiation Data from Satellite Images. Determination of Solar Radiation at Ground Level from Images of the Earth Meteorological Satellites - An Assessment Study. D. Reidel Publishing Company.

Gueymard C.A., 1998. Turbidity determination from Broadband Irradiance measurements: a detailed multi-coefficient approach, *Journal of Applied Meteorology*, Vol. 37, pp 414-435.

Gueymard, C., 2000. Prediction and performance assessment of mean hourly global radiation. *Solar Energy*, Vol.68, No.3, pp. 285-303, 2000.

Ineichen, P., 1983. Quatre années de mesures d'ensoleillement à Genève. Thèse No. 2089, Faculté des sciences de l'Université de Genève.

Kasten F., 1983) Parametrisierung der Globalstrahlung durch Bedeckungsgrad und Trübungsfaktor. *Ann. Met*, 20, 49–50.

Muneer T., 1990. Solar radiation model for Europe. Building Serv. Eng. Res. Technol. 11, 153-163

Molineaux, B, P. Ineichen and Delauney, J.J., 1995. Direct luminous efficacy and atmospheric turbidity – improving model performance. *Solar Energy*, Vol. 55, No. 2, pp. 125-137, 1995.

Page, J., 1996. ESRA Task II Technical Report Number 11. Project Internal.

Perez, R., R. Stewart, C. Arbogast, R. Seals and J. Scott, 1986. An anisotropic hourly diffuse radiation model for sloping surfaces: Description, performance validation, site dependency evaluation. *Solar Energy,* Vol. 36, No. 6, pp. 481-497.

Perez, R., R. Seals, P. Ineichen, R. Stewart and D. Menicucci, 1987. A new simplified version of the Perez Diffuse Irradiance Model for tilted surfaces. *Solar Energy*, Vol. 39, No.3,pp. 221-231.

Perez, R., P. Ineichen, R. Seals, J. Michalsky and R. Stewart, 1990. Modeling daylight availability and irradiance components from direct and global irradiance. *Solar Energy*, Vol. 44, No.5, pp. 271-289.

Perez, R., P. Ineichen, E. Maxwell, R. Seals and A. Zelenka, 1991. Dynamic Models for hourly global-to-

direct irradiance conversion. Edited in: Solar World Congress 1991. Volume 1, Part II. Proceedings of the Biennial Congress of the International Solar Energy Society, Denver, Colorado, USA, 19-23 August 1991.

Remund, J. and S. Kunz, 1995. METEONORM – a comprehensive meteorological database and planning tool for system design. In Proceedings of 13th Solar Energy Photovoltaic Conference and Exhibition, Nice. Commission of the European Communities, CEC). Volume I.

Remund, J. and S. Kunz, 1997. METEONORM Version 3.0. Meteotest, Fabrikstrasse 14, 3012 Bern, Switzerland.

Remund, J. and S. Kunz, 1999. METEONORM Version 4.0. Meteotest, Fabrikstrasse 14, 3012 Bern, Switzerland.

Remund, J., E. Salvisberg and S. Kunz, 1998. Generation of hourly shortwave radiation data on tilted surfaces at any desired location. *Solar Energy*, Vol. 62, No. 5, pp. 331-334,1998.

Rigollier, C., O. Bauer and L. Wald, 2000. On the clear sky model of the ESRA with respect to the heliosat method. *Solar Energy*, Vol.68, No.1, pp.33-48, 2000.

Skartveit, A., J.A.Olseth and M.E.Tuft, 1998. An hourly diffuse fraction model with correction for variability and surface albedo. *Solar Energy*, Vol. 63, No. 3, pp. 173-183, 1998.

Wald L., Albuisson M., Best C., Delamare C., Dumortier D., Gaboardi E., Hammer A., Heinemann D., Kift R., Kunz S., Lefèvre M., Leroy S., Martinoli M., Ménard L., Page J., Prager T., Ratto C., Reise C., Remund J., Rimoczi-Paal A., Van der Goot E., Vanroy F., and Webb A., 2002, SoDa: a project for the integration and exploitation of networked solar radiation databases. In: Environmental Communication in the Information Society, W. Pillmann, K. Tochtermann Eds, Part 2, pp. 713-720. Published by the International Society for Environmental Protection, Vienna, Austria

Remund J., Wald L., Page, J., 2003. Chain of algorithms to calculate advanced radiation parameters. Proceedings of ISES Solar World Congress, 16-19 June, Göteborg, Sweden, CD-ROM published by International Solar Energy Society

ANNEX

For many chain links the clearness index is used. This index is defined by

Monthly daily hourly

$$KT_m = \frac{G_m}{G_{0m}} \qquad KT_d = \frac{G_d}{G_{0d}} \qquad KT_h = \frac{G_h}{G_{0h}} \qquad (A1)$$

Markov Transition Matrices used for generation of daily clearness index (Tab. A1-A9).

Tab. A1: Markov transition matrix for 0.10 <= $KT_{m,c}$<= 0.20

	0.0-0.1	0.1-0.2	0.2-0.3	0.3-0.4	0.4-0.5	0.5-0.6	0.6-0.7	0.7-0.8	0.8-0.9	0.9-1.0
0.0-0.1	0.000	0.000	0.000	0.000	0.000	0.000	0.000	0.000	0.000	0.000
0.1-0.2	0.000	0.000	0.000	0.000	0.000	0.000	0.000	0.000	0.000	0.000
0.2-0.3	0.000	0.000	0.000	0.000	0.000	0.000	0.000	0.000	0.000	0.000
0.3-0.4	0.000	0.000	0.000	0.000	0.000	0.000	0.000	0.000	0.000	0.000
0.4-0.5	0.000	0.000	0.000	0.000	0.000	0.000	0.000	0.000	0.000	0.000
0.5-0.6	0.000	0.000	0.000	0.000	0.000	0.000	0.000	0.000	0.000	0.000
0.6-0.7	0.000	0.000	0.000	0.000	0.000	0.000	0.000	0.000	0.000	1.000
0.7-0.8	0.000	0.000	0.000	0.000	0.000	0.000	0.000	0.000	0.000	0.000
0.8-0.9	0.000	0.000	0.000	0.000	0.000	0.000	0.000	0.000	0.000	0.000
0.9-1.0	0.000	0.000	0.000	0.000	0.000	0.000	0.250	0.000	0.000	0.750

Tab. A2: Markov transition matrix for 0.20 <= $KT_{m,c}$ <= 0.30

	0.0-0.1	0.1-0.2	0.2-0.3	0.3-0.4	0.4-0.5	0.5-0.6	0.6-0.7	0.7-0.8	0.8-0.9	0.9-1.0
0.0-0.1	0.000	0.000	0.000	0.000	0.000	0.000	0.000	0.000	0.000	0.000
0.1-0.2	0.000	0.500	0.167	0.167	0.167	0.000	0.000	0.000	0.000	0.000
0.2-0.3	0.000	1.000	0.000	0.000	0.000	0.000	0.000	0.000	0.000	0.000
0.3-0.4	0.000	0.333	0.000	0.000	0.333	0.000	0.000	0.000	0.000	0.333
0.4-0.5	0.000	1.000	0.000	0.000	0.000	0.000	0.000	0.000	0.000	0.000
0.5-0.6	0.000	0.000	0.000	0.000	0.000	0.000	0.000	0.000	0.000	0.000
0.6-0.7	0.000	0.000	0.000	0.000	0.000	0.000	0.000	0.000	0.000	0.000
0.7-0.8	0.000	0.000	0.000	0.000	0.000	0.000	0.000	0.000	0.000	0.000
0.8-0.9	0.000	0.000	0.000	0.000	0.000	0.000	0.000	0.000	0.000	0.000
0.9-1.0	0.000	0.000	0.000	0.000	0.000	1.000	0.000	0.000	0.000	0.000

Tab. A3:Markov transition matrix for 0.30 <= $KT_{m,c}$ <= 0.40

	0.0-0.1	0.1-0.2	0.2-0.3	0.3-0.4	0.4-0.5	0.5-0.6	0.6-0.7	0.7-0.8	0.8-0.9	0.9-1.0
0.0-0.1	0.133	0.319	0.204	0.115	0.074	0.033	0.030	0.044	0.011	0.037
0.1-0.2	0.081	0.303	0.232	0.127	0.088	0.060	0.029	0.031	0.018	0.033
0.2-0.3	0.036	0.195	0.379	0.135	0.087	0.039	0.042	0.027	0.025	0.036
0.3-0.4	0.032	0.190	0.205	0.189	0.119	0.069	0.059	0.038	0.045	0.054
0.4-0.5	0.051	0.175	0.189	0.185	0.140	0.079	0.060	0.040	0.017	0.064
0.5-0.6	0.042	0.213	0.243	0.126	0.117	0.090	0.045	0.036	0.021	0.069
0.6-0.7	0.017	0.166	0.237	0.141	0.100	0.091	0.054	0.062	0.046	0.087
0.7-0.8	0.038	0.171	0.190	0.133	0.095	0.090	0.057	0.062	0.043	0.119
0.8-0.9	0.044	0.093	0.231	0.143	0.115	0.066	0.038	0.060	0.099	0.110
0.9-1.0	0.029	0.131	0.163	0.127	0.062	0.092	0.065	0.072	0.078	0.180

Tab. A4:Markov transition matrix for 0.40 <= $KT_{m,c}$ <= 0.50

	0.0-0.1	0.1-0.2	0.2-0.3	0.3-0.4	0.4-0.5	0.5-0.6	0.6-0.7	0.7-0.8	0.8-0.9	0.9-1.0
0.0-0.1	0.116	0.223	0.196	0.129	0.093	0.077	0.054	0.044	0.032	0.037
0.1-0.2	0.051	0.228	0.199	0.143	0.101	0.083	0.065	0.052	0.035	0.043
0.2-0.3	0.028	0.146	0.244	0.156	0.120	0.092	0.069	0.053	0.040	0.052
0.3-0.4	0.020	0.111	0.175	0.208	0.146	0.104	0.074	0.067	0.044	0.052
0.4-0.5	0.017	0.115	0.161	0.177	0.155	0.102	0.085	0.067	0.054	0.068
0.5-0.6	0.018	0.114	0.147	0.156	0.142	0.123	0.088	0.075	0.060	0.077
0.6-0.7	0.019	0.116	0.152	0.153	0.133	0.100	0.090	0.078	0.061	0.098
0.7-0.8	0.022	0.105	0.145	0.134	0.112	0.109	0.103	0.085	0.077	0.108
0.8-0.9	0.016	0.100	0.119	0.120	0.100	0.105	0.099	0.096	0.120	0.126
0.9-1.0	0.012	0.081	0.109	0.115	0.101	0.082	0.075	0.091	0.107	0.226

Tab. A5: Markov transition matrix for $0.50 <= KT_{m,c} <= 0.60$

	0.0-0.1	0.1-0.2	0.2-0.3	0.3-0.4	0.4-0.5	0.5-0.6	0.6-0.7	0.7-0.8	0.8-0.9	0.9-1.0
0.0-0.1	0.095	0.201	0.140	0.121	0.112	0.076	0.073	0.066	0.055	0.061
0.1-0.2	0.029	0.176	0.158	0.133	0.121	0.096	0.078	0.079	0.067	0.063
0.2-0.3	0.015	0.096	0.171	0.157	0.139	0.121	0.093	0.080	0.066	0.062
0.3-0.4	0.008	0.055	0.103	0.199	0.186	0.130	0.108	0.085	0.063	0.063
0.4-0.5	0.006	0.039	0.077	0.145	0.236	0.167	0.113	0.083	0.064	0.069
0.5-0.6	0.006	0.044	0.080	0.128	0.192	0.166	0.123	0.100	0.081	0.080
0.6-0.7	0.006	0.049	0.082	0.132	0.152	0.139	0.125	0.110	0.095	0.109
0.7-0.8	0.007	0.047	0.086	0.113	0.138	0.125	0.114	0.124	0.112	0.134
0.8-0.9	0.006	0.048	0.079	0.105	0.120	0.108	0.100	0.120	0.138	0.177
0.9-1.0	0.005	0.033	0.062	0.085	0.102	0.086	0.088	0.103	0.144	0.291

Tab. A6: Markov transition matrix for $0.60 <= KT_{m,c} <= 0.70$

	0.0-0.1	0.1-0.2	0.2-0.3	0.3-0.4	0.4-0.5	0.5-0.6	0.6-0.7	0.7-0.8	0.8-0.9	0.9-1.0
0.0-0.1	0.061	0.169	0.146	0.095	0.106	0.094	0.108	0.085	0.067	0.070
0.1-0.2	0.023	0.113	0.130	0.114	0.107	0.111	0.102	0.108	0.100	0.092
0.2-0.3	0.007	0.062	0.105	0.132	0.151	0.126	0.113	0.106	0.097	0.100
0.3-0.4	0.004	0.026	0.063	0.150	0.189	0.147	0.118	0.108	0.097	0.099
0.4-0.5	0.002	0.017	0.040	0.098	0.230	0.164	0.130	0.111	0.103	0.106
0.5-0.6	0.002	0.016	0.040	0.084	0.162	0.179	0.149	0.129	0.119	0.120
0.6-0.7	0.003	0.018	0.040	0.079	0.142	0.143	0.153	0.140	0.139	0.144
0.7-0.8	0.002	0.017	0.041	0.079	0.126	0.120	0.135	0.151	0.162	0.167
0.8-0.9	0.002	0.017	0.034	0.069	0.108	0.106	0.114	0.144	0.191	0.215
0.9-1.0	0.001	0.012	0.023	0.050	0.083	0.079	0.088	0.118	0.185	0.362

Tab. A7: Markov transition matrix for $0.70 <= KT_{m,c} <= 0.80$

	0.0-0.1	0.1-0.2	0.2-0.3	0.3-0.4	0.4-0.5	0.5-0.6	0.6-0.7	0.7-0.8	0.8-0.9	0.9-1.0
0.0-0.1	0.049	0.091	0.112	0.070	0.098	0.077	0.105	0.119	0.112	0.168
0.1-0.2	0.019	0.070	0.090	0.105	0.119	0.113	0.103	0.134	0.121	0.125
0.2-0.3	0.005	0.028	0.074	0.114	0.130	0.123	0.113	0.118	0.145	0.151
0.3-0.4	0.001	0.011	0.039	0.102	0.169	0.135	0.123	0.126	0.136	0.156
0.4-0.5	0.001	0.007	0.021	0.062	0.175	0.143	0.132	0.137	0.157	0.167
0.5-0.6	0.001	0.007	0.020	0.049	0.117	0.146	0.150	0.157	0.172	0.182
0.6-0.7	0.000	0.005	0.015	0.047	0.097	0.122	0.151	0.169	0.197	0.197
0.7-0.8	0.001	0.006	0.016	0.040	0.084	0.098	0.130	0.179	0.224	0.223
0.8-0.9	0.001	0.005	0.011	0.034	0.067	0.079	0.107	0.161	0.262	0.275
0.9-1.0	0.000	0.003	0.007	0.022	0.045	0.055	0.074	0.112	0.222	0.459

Tab. A8: Markov transition matrix for $0.80 <= KT_{m,c} <= 0.90$

	0.0-0.1	0.1-0.2	0.2-0.3	0.3-0.4	0.4-0.5	0.5-0.6	0.6-0.7	0.7-0.8	0.8-0.9	0.9-1.0
0.0-0.1	0.000	0.000	0.077	0.077	0.154	0.077	0.154	0.154	0.077	0.231
0.1-0.2	0.000	0.043	0.061	0.070	0.061	0.087	0.087	0.217	0.148	0.226
0.2-0.3	0.000	0.017	0.042	0.073	0.095	0.112	0.120	0.137	0.212	0.193
0.3-0.4	0.001	0.003	0.015	0.055	0.106	0.091	0.120	0.139	0.219	0.250
0.4-0.5	0.000	0.002	0.009	0.035	0.097	0.113	0.123	0.155	0.209	0.258
0.5-0.6	0.000	0.002	0.007	0.028	0.063	0.089	0.123	0.157	0.235	0.295
0.6-0.7	0.000	0.002	0.005	0.020	0.054	0.069	0.114	0.170	0.260	0.307
0.7-0.8	0.000	0.001	0.004	0.015	0.043	0.058	0.097	0.174	0.288	0.320
0.8-0.9	0.000	0.001	0.002	0.011	0.027	0.039	0.071	0.139	0.319	0.390
0.9-1.0	0.000	0.001	0.001	0.005	0.015	0.024	0.043	0.086	0.225	0.600

Tab. A9: Markov transition matrix for $0.90 <= KT_{d,c} <= 1.00$

	0.0-0.1	0.1-0.2	0.2-0.3	0.3-0.4	0.4-0.5	0.5-0.6	0.6-0.7	0.7-0.8	0.8-0.9	0.9-1.0
0.0-0.1	0.000	0.000	0.000	0.000	0.000	0.000	0.000	0.000	0.000	0.000
0.1-0.2	0.000	0.000	0.000	0.000	0.000	0.000	0.000	0.000	0.000	0.000
0.2-0.3	0.000	0.000	0.000	0.000	0.000	0.000	0.333	0.333	0.000	0.333
0.3-0.4	0.000	0.000	0.000	0.000	0.048	0.000	0.143	0.095	0.190	0.524
0.4-0.5	0.000	0.000	0.014	0.000	0.027	0.041	0.041	0.233	0.192	0.452
0.5-0.6	0.000	0.000	0.000	0.008	0.039	0.031	0.078	0.093	0.326	0.426
0.6-0.7	0.000	0.000	0.000	0.006	0.019	0.019	0.067	0.102	0.254	0.533
0.7-0.8	0.000	0.000	0.000	0.005	0.012	0.024	0.041	0.106	0.252	0.560
0.8-0.9	0.000	0.000	0.000	0.001	0.006	0.012	0.031	0.078	0.283	0.589
0.9-1.0	0.000	0.000	0.000	0.001	0.002	0.004	0.012	0.029	0.134	0.817